ACI MATERIALS JOURNAL TECHNICAL PAPER

Title No. 121-M30

Three-Stage Testing Protocol to Recreate Thermomechanical Properties of Mass Concrete

by A. S. Carey, G. B. Sisung, I. L. Howard, B. Songer, D. A. Scott, and J. Shannon

Determining the in-place properties of mass concrete placements is elusive, and currently there are minimal to no test methods available that are both predictive and a direct measurement of mechanical properties. This paper presents a three-stage testing framework that uses common laboratory equipment and laboratory-scale specimens to quantify thermal and mechanical properties of mass high-strength concrete placements. To evaluate this framework, four mass placements of varying sizes and insulations were cast, and temperature histories were measured at several locations within each placement, where maximum temperatures of 107 to 119°C (225 to 246°F) were recorded. The laboratory curing protocols were then developed using this mass placement temperature data and the three-stage testing framework to cure laboratory specimens to represent each mass placement. Laboratory curing protocols developed for center and intermediate regions of the mass placements reasonably replicated thermal histories of the mass placements, while the first stage of the three-stage framework reasonably replicated temperatures near the edge of the mass placements. Additionally, there were statistically significant relationships detected between calibration variables used to develop laboratory curing protocols and measured compressive strength. Overall, the proposed three-stage testing framework is a measurable step toward creating a predictive laboratory curing protocol by accounting for the mixture characteristics of thermomechanical properties of high-strength concretes.

Keywords: high-strength concrete (HSC); insulated curing block; mass placements; programmable environmental chamber.

INTRODUCTION AND BACKGROUND

There have been several attempts to quantify the in-place properties of mass concrete placements using nondestructive test methods presented by ACI Committee 228,[1-5] as well as numerical techniques to quantify complex chemical reactions to predict time-temperature profiles and subsequent mechanical properties.[6] Several methodologies have been developed and studied over time to better understand thermomechanical properties of mass placements, such as cast-in-place cylinders (ASTM C873/C873M-15), the maturity method (ASTM C1074-19), temperature-matched curing (BS 1881-130), and numerical analysis techniques. These methods generally aim to predict the relationship between time-temperature history and mechanical properties in a nondestructive manner. Carey et al.[7] provided an in-depth review of each of these methodologies with respect to quantifying temperature development and mechanical properties in mass placements. A comparison of these methods found that none were both predictive and a direct measure of mechanical properties in the presence of anticipated thermal conditions.

The authors have been developing a testing framework over a multi-year period that is intended to fill this gap. Initial efforts aimed to evaluate the feasibility of using common laboratory equipment to cure 10.2 x 20.3 cm (4 x 8 in.) cylindrical specimens in a similar time-temperature history to modest and mass placements. For modest placements, laboratory curing protocols using a programmable bath and insulating block were successful for placements with a minimum least dimension of 0.15 m (0.5 ft), which were large enough to overcome the influence of environmental conditions by generating a substantial amount of heat.[8] For an insulated mass placement with a diameter of 1.8 m (6 ft) and height of 1.3 m (4 ft), an average internal peak temperature of 94°C (201°F) was produced, and laboratory specimens cured using a programmable bath and insulating block were able to reasonably replicate the time-temperature profile while also reaching a peak temperature of 92°C (198°F).[9] Based on these initial findings, efforts have focused on developing a three-stage testing protocol where thermal histories of mass placements could be recreated using common laboratory equipment to cure laboratory specimens, where the effects of mixture constituents on thermal properties are considered during the development of the laboratory curing protocol (Fig. 1).

RESEARCH SIGNIFICANCE

Determining the in-place properties of mass placements is elusive, and currently there are minimal to no test methods available that are both predictive and a direct measurement of mechanical properties in the presence of anticipated thermal conditions. The authors have developed a testing framework that has the potential to fill this gap in available testing methods. This paper serves as a proof of concept for a three-stage curing procedure initially presented in Carey et al.[7] that is a measurable step toward making the proposed laboratory testing protocols predictive by accounting for individual mixture characteristics of the thermomechanical properties of high-strength concretes (HSCs).

USE OF HIGH-STRENGTH CONCRETE IN MASS PLACEMENTS

In recent years, the use of HSC in larger to mass placements has increased as the need to improve mechanical

ACI Materials Journal, V. 121, No. 3, May 2024.
MS No. M-2023-276.R1, doi: 10.14359/51740705, received May 7, 2023, and reviewed under Institute publication policies.

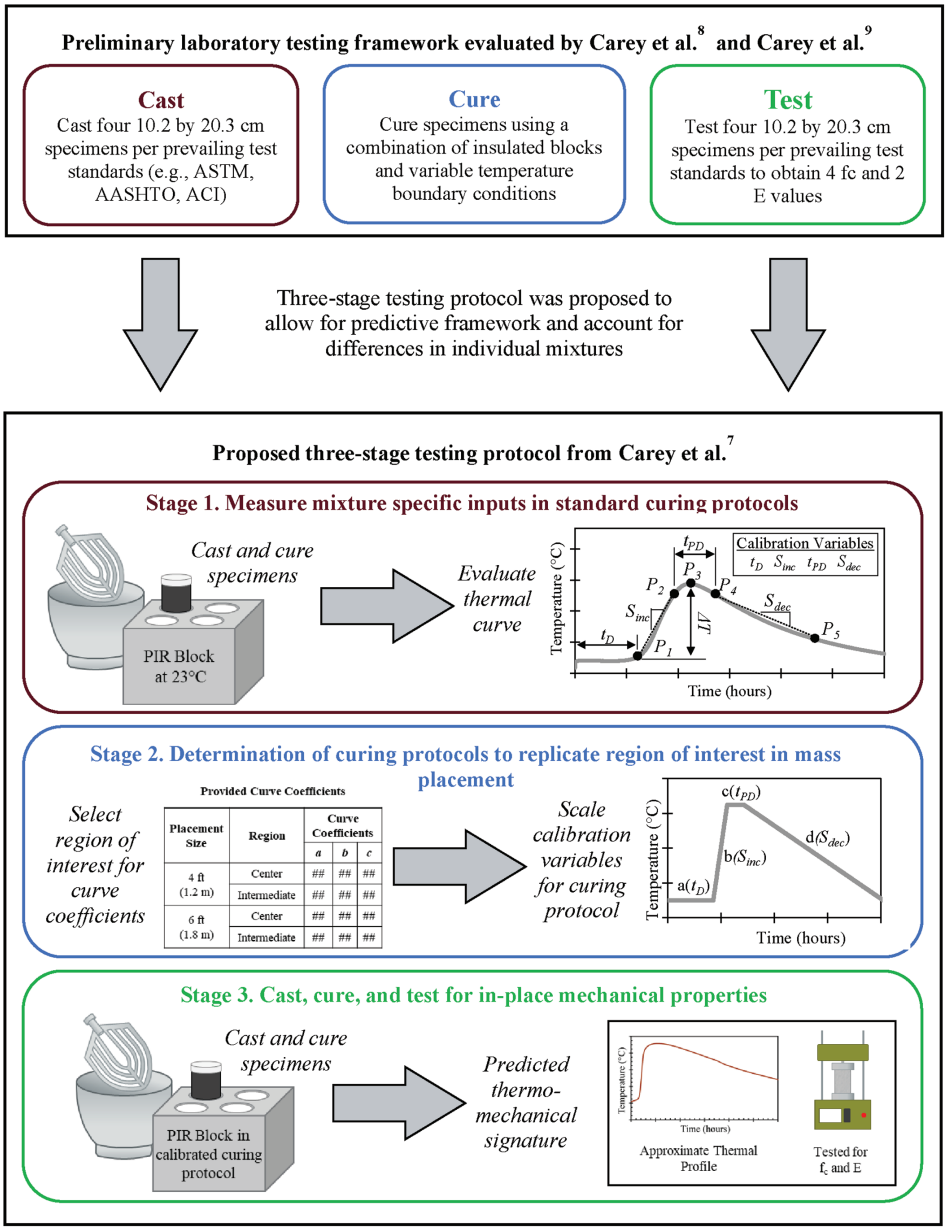

Fig. 1—Summary of preliminary testing framework and proposed three-stage testing protocol. (Note: °F = (9/5)(°C) + 32.)

properties (for example, compressive and tensile strength and durability) has grown. A recent survey of state Departments of Transportation (DOTs) found that, as of 2019, four states routinely use ultra-high-performance concrete (UHPC) in full-scale structural applications, while 15 commonly use UHPC in joints and connections.[10] Scenarios where one may consider using UHPC or HSC in a mass placement include protective structures, retrofitting critical infrastructure elements, and construction in areas where high durability is a first-order consideration (for example, coastal construction). As the development of nonproprietary UHPC mixtures that are usually more economical than proprietary mixtures continues to progress, it is anticipated that more DOTs will begin to use UHPC in their day-to-day construction activities.

When using HSCs with increased cementitious materials contents, internal temperatures often far exceed those of traditional ready mixed concrete (RMC) placements. Table 1 summarizes reported peak temperatures of HSC mass placements.[9,11-15] HSC mass placements evaluated in Table 1 reported a typical maximum temperature of 90°C (194°F), which is similar to the recommended curing temperatures in ASTM C1856/C1856M-17 for mixtures with metallic fibers.[16] Table 1 also reports external temperatures of large, thin slabs and modestly sized columns ranging from 54 to 64°C (129 to 147°F). Though these temperatures were noticeably lower than other Table 1 HSC mass placements where internal temperatures were reported, these external temperatures were comparable to internal temperatures of RMC mass placements.[17,18] While most mass HSC placements exceeded the maximum internal temperature of 70°C (158°F) as defined by ACI PRC-207.1-21,[19] the threat of delayed ettringite formation (DEF) is minimal as the water-cementitious materials ratio (*w*/*cm*) is typically below 0.20 and the system has low permeability due to its tight microstructure.[20,21] In other words, for mass placements

Table 1—Summary of HSC placements reported in literature

Reference	Placement size	Insulation?	Total cementitious materials, kg/m^3	Reported T_{max}, °C
Kodur et al.[11]	1 m cube	Yes	480.6 I/II + 211.5 SF + 96.1 FA + 173 LSP = 961.2	90
Kodur et al.[11]	1 m cube	No	480.6 I/II + 211.5 SF + 96.1 FA + 173 LSP = 961.2	86
Kodur et al.[11]	1 m cube	No	480.6 I/II + 297.6 SF + 173 LSP = 961.2	96
Sbia et al.[12]	1 m cube	Yes	480.6 I/II + 211.5 SF + 96.1 slag + 173 LSP = 961.2	90
Li et al.[13]	6 x 10 x 2.5 m bridge element	Yes	700 I/II + 100 SF + 200 LSP = 1000	90
Carey et al.[9]	1.8 x 1.3 m column	Yes	732 CH + 126 SF + 82 FA = 940	99
Soliman et al.[14]	4.9 x 1.5 x 0.075 m arch slab	No	549 I/II + 204 SF + 403 GP = 1156	54
Aghdasi et al.[15]	0.7 x 0.7 x 1.1 m column	No	1 part I/II + 0.1 part FA + 0.25 part SF + 0.25 part GP	64

Note: I/II is ASTM C150 Type I/II cement; SF is silica fume; FA is fly ash; LSP is limestone powder; GP is glass powder; CH is Class H cement; all reported T_{max} were measured at center of placement, except for Carey et al.,[9] measured at an intermediate location, and Aghdasi et al.,[15] measured at the surface. 1 m = 3.28 ft; 1 kg/m^3 = 1.69 lb/yd^3; °F = (9/5) (°C) + 32.

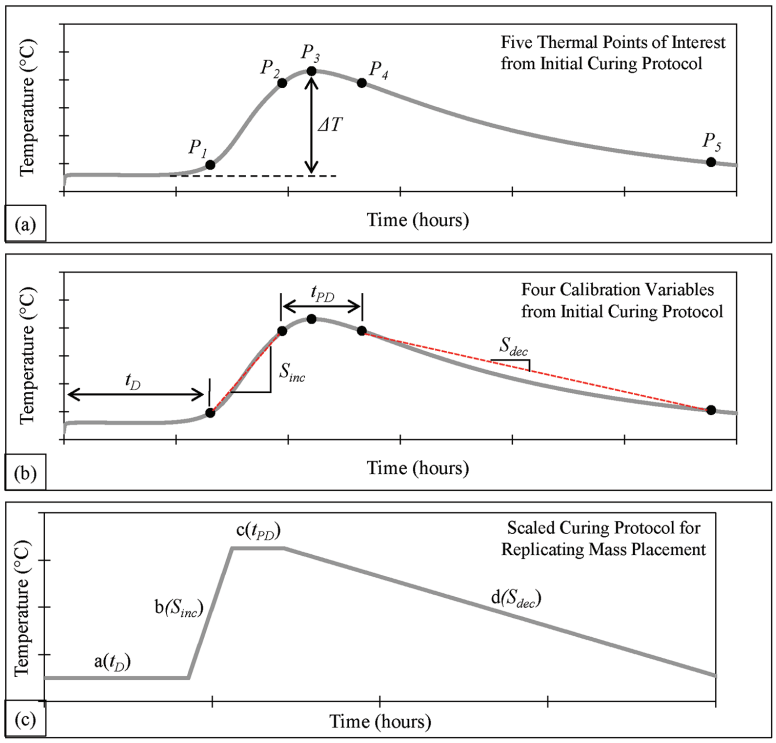

Fig. 2—Development of boundary conditions using proposed three-stage protocol. (Note: °F = (9/5)(°C) + 32.)

where HSC mixtures are used, the deleterious effects of DEF are a secondary concern.

EXPERIMENTAL PROGRAM

Description of three-stage testing protocol

As outlined in Fig. 1, the proposed three-stage testing protocol uses an initial curing regime that measures mixture-specific variables (Stage 1), scales these variables using constants derived from available mass placement data (Stage 2), and then cures specimens using a regime intended to simulate the temperature history of a mass placement (Stage 3). The Stage 1 initial curing protocol uses an insulated curing block to cure hydrating concrete specimens in a variable temperature (VT) bath (or equivalent) programmed to remain at 23°C (73°F). After 3 days of curing, where the temperature surrounding the block remains at 23°C (73°F), the resulting thermal curve is evaluated to determine five thermal points of interest (TPOIs) (Fig. 2(a)). First, maximum temperature (T_{max}) is calculated and reported as P_3. The difference between P_3 and the initial test temperature is then reported as ΔT. P_1 can then be calculated as the point where the temperature begins increasing by more than 5% of ΔT over a 30-minute period, while P_2 is the point where the temperature no longer increases by 5% of ΔT over a 30-minute period. P_4 and P_5 are then reported as the times after peak temperature (P_3) that correspond to temperature values of P_2 and P_1, respectively. Using these five TPOIs, calibration variables are then calculated and are visually defined in Fig. 2(b). Dormant period length (t_D) is calculated as the total time from the start of thermal curing to P_1. Peak temperature dormant period (t_{PD}) is calculated as the time between P_2 and P_4. Rate of temperature increase (S_{inc}) is calculated as the linear slope between P_1 and P_2, while rate of temperature decrease (S_{dec}) is calculated as the linear slope between P_4 and P_5.

Table 2—High-strength mixture batching quantities

Constituent	Specific gravity	Laboratory quantity	Field quantity
Type I/II cement, kg/m^3 (lb/yd^3)	3.15	854 (1440)	854 (1440)
Silica fume, kg/m^3 (lb/yd^3)	2.25	163 (275)	163 (275)
Metakaolin, kg/m^3 (lb/yd^3)	2.60	22 (37)	22 (37)
Manufactured sand, kg/m^3 (lb/yd^3)	2.74	581 (979)	587 (990)
Natural sand, kg/m^3 (lb/yd^3)	2.63	561 (946)	564 (950)
HRWRA, mL/kg (oz./lb)	1.08	23.0 (0.35)	23.0 (0.35)
Retarder, mL/kg (oz./lb)	1.08	1.3 (0.02)	1.3 (0.02)
Defoamer, % weight of water	1.08	0.14	0.08
Water, kg/m^3 (lb/yd^3)	1.00	179 (301)	170 (287)
w/cm	—	0.16	0.16

Note: Laboratory mixtures used oven-dry aggregate, while field mixtures accounted for water during batching process; HRWRA and retarder dosage rates are reported as volume per weight of cementitious materials.

Stage 2 of the Fig. 1 testing protocol scales calibration variables by a set of constants to produce a thermal curing protocol that can be programmed into an environmental chamber to cure laboratory-scale specimens using a time-temperature history that is similar to a mass concrete placement (Fig. 2(c)). Currently, these scaling constants are not fully defined by the authors and will require additional data sets to fully develop. It is ultimately envisioned for scaling constants representative of given mass placement scenarios to be provided to users of the three-stage testing protocol so the framework can be predictive. However, because this paper serves as a proof of concept for the three-stage testing protocol, scaling constants were calculated by dividing calibration variables from each thermocouple (TC) in each mass placement by the calibration variables of the Stage 1 time-temperature profile. Because scaling coefficients were calculated using mass placement data, generated laboratory protocols used in Stage 3 of the Fig. 1 testing protocol should produce time-temperature profiles in laboratory specimens that closely follow those of the mass placements. If the generated laboratory protocols do not yield similar time-temperature profiles, then the proposed framework is not feasible.

Materials

Experiments were conducted on an HSC developed by the U.S. Army Corps of Engineers (Table 2). An ASTM C150 Type I/II cement with a Blaine fineness of 450 m^2/kg (2197 ft^2/lb) was used. Silica fume had a bulk density ranging from 500 to 700 kg/m^3 (843 to 1180 lb/yd^3) and a SiO_2 content of at least 85%. Metakaolin conforming to ASTM C618 had a bulk density of 400 kg/m^3 (674 lb/yd^3) with SiO_2 contents ranging from 51 to 53% and Al_2O_3 ranging from 42 to 44%. Two sands were used: a manufactured granite sand with a water absorption of 1.0% and fineness modulus of 2.69, and a natural sand with a water absorption of 0.5% and a fineness modulus of 2.32. The gradation of each sand is shown in Fig. 3. Coarse aggregates are typically not used in HSC and UHPC mixtures. For laboratory mixtures, aggregates

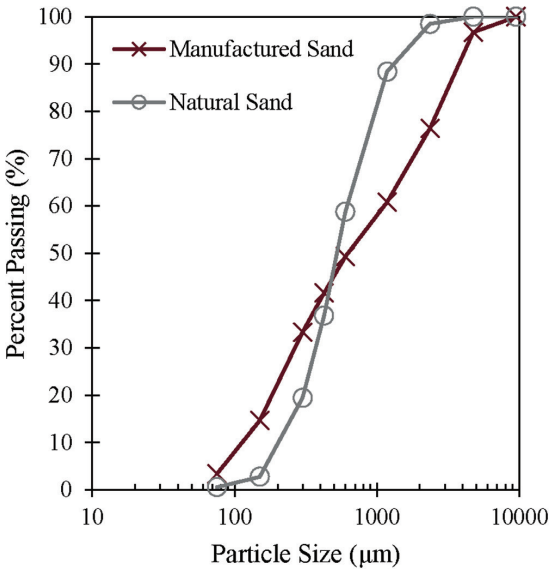

Fig. 3—Gradation of manufactured and natural sand. (Note: 1 μm = 3.93 × 10^{-5} in.)

were air-dried for several weeks and reached uniform moisture contents of 0.5% for manufactured sand and <0.1% for natural sand. For field mixtures, aggregate moisture contents were taken during batching to reach the desired *w/cm*. Three admixtures were used: a high-range water-reducing admixture (HRWRA), a defoamer, and a set retarder.

Mass placement preparation and curing environment

Four mass placements were cast at a facility in south Mississippi in June 2018. Four metal culverts with a wall thickness of 6.4 mm (0.25 in.) and a 12.7 mm (0.50 in.) piece of metal attached to the bottom served as formwork (Fig. 4(a)). Two placements were 1.22 m (4 ft) in diameter and height, while the other placements were 1.83 m (6 ft) in diameter and height. Ten TCs were placed in each culvert at known locations to measure temperature (Fig. 4(b)). TCs were attached to a metal frame that was secured at the center of the placement prior to casting. One placement of each size was fully wrapped in an insulating blanket immediately after casting for the duration of hydration. All placements were cured in an open-ended hangar (that is, they were covered from rain and direct sunlight but not temperature-controlled). TCs were placed next to each placement to record ambient temperature profiles. When the TCs were compared to local weather records, the open-ended hangar did minimize large ambient temperature changes due to daily temperature fluctuations, as typical daily temperature fluctuation was 8.8°C (15.8°F), while the temperature fluctuation inside the facility was 4.3°C (7.7°F).

Laboratory-scale specimen preparation and curing environment

Laboratory mixing occurred at Mississippi State University (MSU) using a benchtop mixer with a paddle attachment to induce shear mixing. Cement, silica fume, metakaolin, manufactured sand, and natural sand were mixed for 1 minute to create a homogenous mixture. 80% of the water

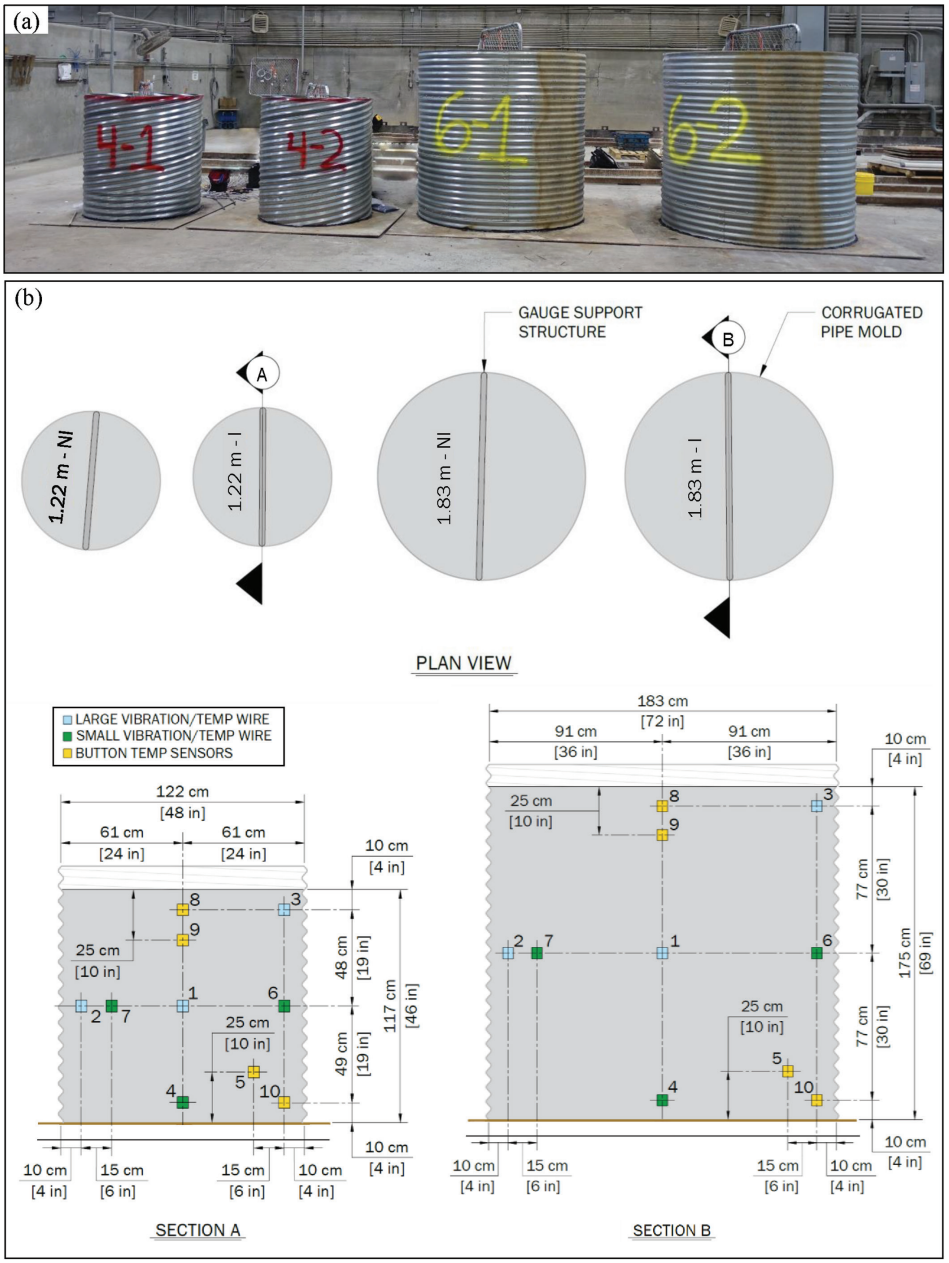

Fig. 4—(a) Mass placements formwork at testing location; and (b) schematic of thermocouple locations. (Note: 1 m = 3.28 ft.)

was added to premixed materials and mixed at a low speed for 1 minute. After 1 minute, the remaining 20% of water, HRWRA, defoamer, and set retarder were added and mixed at an increased mixing speed until a fluid state was achieved. Two 10.2 x 20.3 cm (4 x 8 in.) plastic cylinder molds were filled in two equal lifts and externally vibrated between lifts to remove air voids. After the first lift, a TC was placed in the middle of one of the two specimens. Two mixtures were mixed simultaneously to produce four 10.2 x 20.3 cm (4 x 8 in.) specimens. Once mixed and molded, groups of four specimens were placed in a designated curing environment.

Nineteen curing protocols with varying combinations of insulating block and programmed boundary conditions were used (Table 3). All curing protocols used a VT curing bath that was programmed to alter the air temperature surrounding an insulated curing block (Fig. 5). The VT curing bath consisted of an off-the-shelf concrete curing box that was modified to include a high-temperature water pump, and a programmable temperature controller. This VT curing bath could be replaced with fully commercially available equipment in the future, but it was used herein for continuity with past work (that is, Allard et al.[22] and Carey et al.[8,9]) where previous iterations of the framework have been evaluated. Curing blocks made of polyisocyanurate (PIR; *R*-value = 1.06 m^2·K/W) and aluminum honeycomb (AH; *R*-value = 0.01 m^2·K/W) were used to insulate concrete specimens and were previously used in Carey et al.[9] (Fig. 5).

Of the 15 boundary conditions used in this study, three were recommended in previous studies and are repeated herein for continuity and to evaluate their viability with a different mixture. Carey et al.[8] recommended two protocols for modest placements with least dimensions of 0.15 to 0.50 m (0.5 to 1.6 ft), while Carey et al.[9] recommended a protocol for intermediate regions of an insulated 1.83 m (6 ft)

Table 3—Summary of laboratory curing protocols

Curing protocol	Insulator	Programmed boundary condition				Curing protocol objective
		t_D, hours	S_{inc}, °C/h	t_{PD}, hours	S_{dec}, °C/h	
1	AH	6.0	3.0	4.0	–1.0	Recommended in Carey et al.[8]
2	PIR	—	—	—	—	Recommended in Carey et al.[8]
3	PIR	6.0	11.2	4.0	–0.45	Recommended in Carey et al.[9]
4	PIR	12.5	13.9	25.5	–0.87	Replicate 1.2 m non-insulated placement; R1
5	PIR	13.1	12.3	12.4	–0.77	Replicate 1.2 m non-insulated placement; R2
6	PIR	14.4	8.9	7.3	–0.57	Replicate 1.2 m non-insulated placement; R3
7	AH	14.4	8.9	7.3	–0.57	Replicate 1.2 m non-insulated placement; R3
8	PIR	10.4	14.7	27.4	–0.56	Replicate 1.2 m insulated placement; R1
9	PIR	10.9	13.6	15.6	–0.51	Replicate 1.2 m insulated placement; R2
10	PIR	12.0	10.4	29.3	–0.40	Replicate 1.2 m insulated placement; R3
11	AH	12.0	10.4	29.3	–0.40	Replicate 1.2 m insulated placement; R3
12	PIR	9.8	17.0	50.3	–0.54	Replicate 1.8 m non-insulated placement; R1
13	PIR	9.8	13.8	11.5	–0.48	Replicate 1.8 m non-insulated placement; R2
14	PIR	11.0	6.7	4.0	–0.32	Replicate 1.8 m non-insulated placement; R3
15	AH	11.0	6.7	4.0	–0.32	Replicate 1.8 m non-insulated placement; R3
16	PIR	11.8	15.9	64.5	–0.40	Replicate 1.8 m insulated placement; R1
17	PIR	12.2	13.8	33.7	–0.36	Replicate 1.8 m insulated placement; R2
18	PIR	13.0	6.3	4.5	–0.21	Replicate 1.8 m insulated placement; R3
19	AH	13.0	6.3	4.5	–0.21	Replicate 1.8 m insulated placement; R3

Note: t_D is length of dormant period; S_{inc} is rate of temperature increase; t_{PD} is length of peak temperature; S_{dec} is rate of temperature decrease; boundary condition variables visually defined in Fig. 5; all laboratory experiments were conducted in variable temperature bath; °F = (9/5)(°C) + 32; 1 m = 3.28 ft.

diameter mass placement. The remaining 12 boundary conditions were developed using the three-stage testing protocol and mass placement time-temperature data presented in this paper. Boundary conditions developed in previous efforts were focused on replicating a specific time-temperature profile and were programmed to directly replicate placement temperature profiles. The 12 boundary conditions developed in this paper are the first research activity in evolving toward a predictive testing framework that can generate curing protocols that replicate mass placement temperatures.

Mechanical testing methods

Prior to testing, specimens were ground to obtain plain ends. Compressive strength (f_c) tests for concrete specimens were conducted following ASTM C39/C39M, where specimens were loaded at a rate of 0.24 MPa/s (35 psi/s) until failure. Elastic modulus (E) tests used a linear variable displacement transducer (LVDT) to measure vertical displacement per ASTM C469. An average of two f_c values from identically cured concrete specimens were used to find 40% of the maximum load. E tests were then conducted on the two remaining specimens, which were then tested for f_c, for a total of four f_c and two E per set of four concrete specimens.

RESULTS AND DISCUSSION

Analysis of mass placement time-temperature histories

Time-temperature histories were recorded for each mass placement and are shown in Fig. 6. Temperature trends were expected as increasing placement size and the inclusion of insulation yielded higher peak temperatures. Figure 6 temperatures were all noticeably higher than the peak temperatures reported in Table 1. TPOIs and calibration variables were calculated for each recorded time-temperature history in each mass placement (Table 4). Using Table 4 data and trends in Fig. 5, similar temperature profiles were grouped together to create three temperature regions within each mass placement. Region 1 (R1) was the hottest temperatures (typically at the center of each mass placement), Region 2 (R2) was intermediate temperatures, and Region 3 (R3) was typically temperatures at the edge of each mass placement. Regions were checked using two-tailed t-tests assuming unequal variance at a 0.05 significance level to ensure key variables in each region were different from one another. In other words, R2 was statistically compared to R1 and R3 for each placement. As seen in Fig. 7, there were only three cases where, statistically, there was no difference between variables in two temperature regions: 1) S_{dec} between R1 and R2 in the 1.22 m (4 ft) insulated placement; 2) S_{inc} between R2 and R3 in the 1.83 m (6 ft) non-insulated placement; and 3) S_{dec} between R2 and R3 in the 1.83 m (6 ft) non-insulated placement. In these cases,

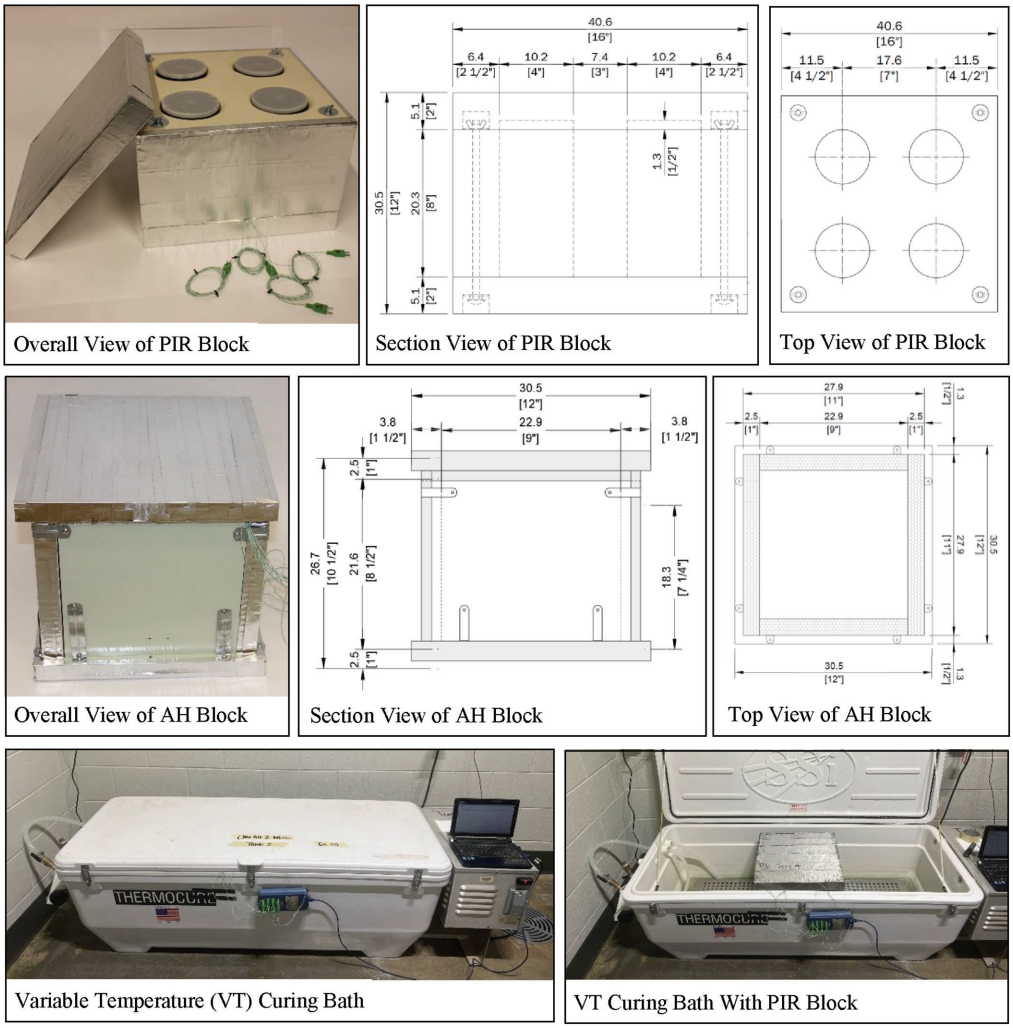

Fig. 5—Insulators and environmental chambers used in study. (Note: Dimensions of curing blocks given in cm [in.].)

visual evaluations of the time-temperature histories justified temperature region grouping.

Analysis of variance (ANOVA) was used to assess overall trends of these mass placements (that is, considering all TCs in each placement regardless of region) at a 0.05 significance level. T_{max} and S_{inc} values (that is, variables defining the time-temperature curve up to peak temperature) were not statistically different between any of the placements reporting *p*-values of 0.39 and 0.37, respectively. However, S_{dec} values of each placement were statistically different from one another with a *p*-value less than 0.01. Additionally, the 1.83 m (6 ft) insulated placement was compared to a placement of the same size and insulation reported in Carey et al.,[9] where a different mixture was used. T_{max} and S_{inc} values were meaningfully different between the placement presented herein (101.1°C and 13.2°C/h [214°F and 23.8°F/h]) and the Carey et al.[9] placement (94.1°C and 3.4°C/h [201.4°F and 6.1°F/h]). However, when evaluating S_{dec}, the two placements were nearly identical (–0.35°C/h [–0.63°F/h] for the placement herein and –0.34°C/h [–0.61°F/h] for the Carey et al.[9] placement). This indicates that mixture characteristics influence initial time-temperature characteristics such as T_{max} and S_{inc}, while the size and insulation of mass placements drive time-temperature histories after peak temperatures have occurred (that is, S_{dec}).

Evaluating feasibility of three-stage testing framework

Figure 8 and Table 5 summarize all data from laboratory-scale specimens that were cured following Table 3 curing protocols. Generally speaking, curing protocols for most center and intermediate regions (that is, R1 and R2) yielded time-temperature profiles that closely resembled mass placements, while the edge region profiles (that is, R3) greatly overestimated mass placement temperatures. R1 protocols produced reasonable time-temperature profiles for 1.22 m (4 ft) placements; however, for the 1.83 m (6 ft) placements, protocols were not successfully implemented due to equipment limitations and extreme temperature ranges. In the 1.83 m (6 ft) non-insulated placement, programmed temperatures exceeded the operating temperature of the VT bath, causing equipment failure, while the combination of VT bath and insulating block could not reach the target temperature for the 1.83 m (6 ft) insulated placement. Further improvements to the proposed three-stage testing protocols are envisioned where equipment with increased

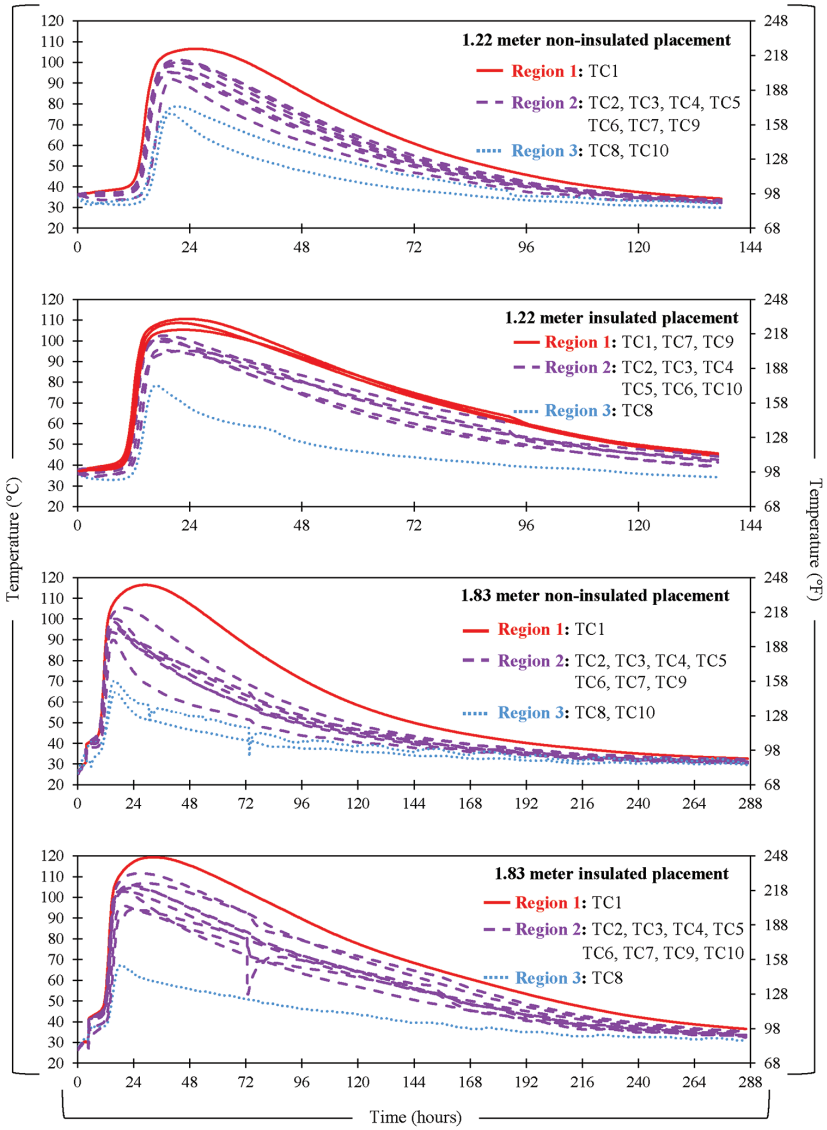

Fig. 6—Recorded time-temperature histories of each mass placement. (Note: 1 m = 3.28 ft.)

operating temperatures is used (for example, programmable ovens in place of a programmable cooler).

R2 protocols produced temperatures that were visually similar to each mass placement. ANOVA testing at a significance level of 0.05 was conducted to compare R2 laboratory curing protocols to mass placements. S_{inc} of the laboratory protocols was significantly different than all four mass placements (p-value <0.01 in all cases), even though programmed S_{inc} rates were the same as each mass placement. This indicates that heat generated by laboratory specimens during hydration increases S_{inc} values to be higher than programmed. T_{max} was significantly different for the 1.22 m (4 ft) insulated placement (p-value of 0.01) and the 1.83 m (6 ft) non-insulated placement (p-value of 0.02), but statistically the same in the 1.22 m (4 ft) non-insulated placement (p-value of 0.13) and 1.83 m (6 ft) insulated placement (p-value of 0.38). The differences in T_{max} for some placements were likely influenced by the meaningfully higher S_{inc} values of laboratory specimens. There was no statistical difference between S_{dec} of laboratory protocols and mass placements (p-values of 0.31, 0.26, 0.08, and 0.47). Although there are some statistical differences in thermal variables between mass placements and laboratory curing protocols, visually, the laboratory protocols reasonably represented mass placement time-temperature profiles. This is considerable evidence of the validity of the three-stage curing protocol concept to recreate mass placement temperature profiles of laboratory specimens.

In addition to the three-stage laboratory protocols developed and evaluated herein, previously recommended curing protocols were also evaluated for continuity with previous efforts. Carey et al.[9] recommended a laboratory protocol to replicate temperatures within an intermediate region of a 1.83 m (6 ft) insulated mass placement. This recommended protocol was developed using one mixture and does not account for changes in mixture constituents. ANOVA testing showed that although T_{max} were statistically the same between the mass placement and laboratory specimens (p-value of 0.14), S_{inc} and S_{dec} were statistically different (p-value <0.01 in both cases). Unlike the recommended protocol from Carey et al.[9] that was developed

Table 4—Calibration variables and scaling constants of mass placements and initial PIR test

Thermal data set	TC	Calibration variables				Scaling constants			
		t_D	S_{inc}	t_{PD}	S_{dec}	a	b	c	d
PIR	—	20.1	9.8	1.4	–1.3	—	—	—	—
1.22 m non-insulated mass placement	1	12.5	13.9	25.5	–0.87	0.62	1.42	18.09	0.69
	2	13.3	12.3	8.8	–0.76	0.66	1.26	6.21	0.60
	3	14.0	11.6	5.0	–0.71	0.70	1.19	3.55	0.57
	4	13.0	11.8	12.3	–0.74	0.65	1.20	8.69	0.59
	5	12.8	12.2	15.3	–0.81	0.63	1.24	10.82	0.65
	6	13.0	12.5	12.0	–0.78	0.65	1.28	8.51	0.62
	7	12.8	12.4	16.3	–0.80	0.63	1.27	11.52	0.64
	8	14.8	9.3	3.3	–0.59	0.73	0.95	2.30	0.47
	9	13.0	13.0	17.3	–0.79	0.65	1.32	12.23	0.63
	10	14.0	8.6	11.3	–0.55	0.70	0.88	7.98	0.43
1.22 m insulated mass placement	1	10.3	15.2	27.0	–0.60	0.51	1.56	19.15	0.48
	2	10.8	14.6	15.8	–0.53	0.53	1.49	11.17	0.42
	3	11.5	13.4	12.5	–0.45	0.57	1.37	8.87	0.36
	4	10.3	13.4	13.3	–0.55	0.51	1.36	9.40	0.44
	5	10.5	13.0	11.8	–0.55	0.52	1.33	8.33	0.44
	6	11.0	14.6	14.3	–0.50	0.55	1.49	10.11	0.40
	7	10.3	14.3	26.0	–0.55	0.51	1.46	18.44	0.44
	8	12.0	10.4	3.0	–0.40	0.60	1.07	2.13	0.32
	9	10.8	14.6	29.3	–0.53	0.53	1.49	20.74	0.42
	10	11.3	12.5	26.3	–0.45	0.56	1.27	18.62	0.36
1.83 m non-insulated mass placement	1	9.8	17.0	50.3	–0.54	0.48	1.73	35.64	0.43
	2	10.0	13.9	8.5	–0.48	0.50	1.42	6.03	0.38
	3	10.3	11.9	3.5	–0.47	0.51	1.22	2.48	0.38
	4	9.3	12.9	14.3	–0.45	0.46	1.32	10.11	0.36
	5	9.5	14.5	10.5	–0.56	0.47	1.48	7.45	0.45
	6	10.0	14.3	8.0	–0.47	0.50	1.46	5.67	0.38
	7	9.8	15.5	25.0	–0.52	0.48	1.58	17.73	0.41
	8	11.3	5.6	4.3	–0.39	0.56	0.57	3.01	0.31
	9	9.8	13.4	10.5	–0.41	0.48	1.37	7.45	0.33
	10	10.8	7.7	3.8	–0.25	0.53	0.79	2.66	0.20
1.83 m insulated mass placement	1	11.8	15.9	64.5	–0.40	0.58	1.63	45.74	0.31
	2	12.0	14.4	32.0	–0.39	0.60	1.47	22.70	0.31
	3	12.8	12.8	21.5	–0.32	0.63	1.30	15.25	0.26
	4	11.8	14.4	22.5	–0.35	0.58	1.47	15.95	0.28
	5	11.8	13.5	16.0	–0.38	0.58	1.38	11.35	0.30
	6	12.3	14.5	31.8	–0.39	0.61	1.48	22.52	0.31
	7	11.8	14.9	47.5	–0.40	0.58	1.52	33.69	0.31
	8	13.0	6.3	4.5	–0.21	0.65	0.64	3.19	0.17
	9	12.0	13.9	56.5	–0.36	0.60	1.42	40.07	0.29
	10	13.3	11.8	41.5	–0.32	0.66	1.20	29.43	0.26

Note: t_D reported in hours; S_{inc} reported in °C/h, t_{PD} reported in hours; S_{dec} reported in °C/h; a, b, c, and d are scaling factors; 1 m = 3.28 ft; °F = (9/5)(°C) + 32.

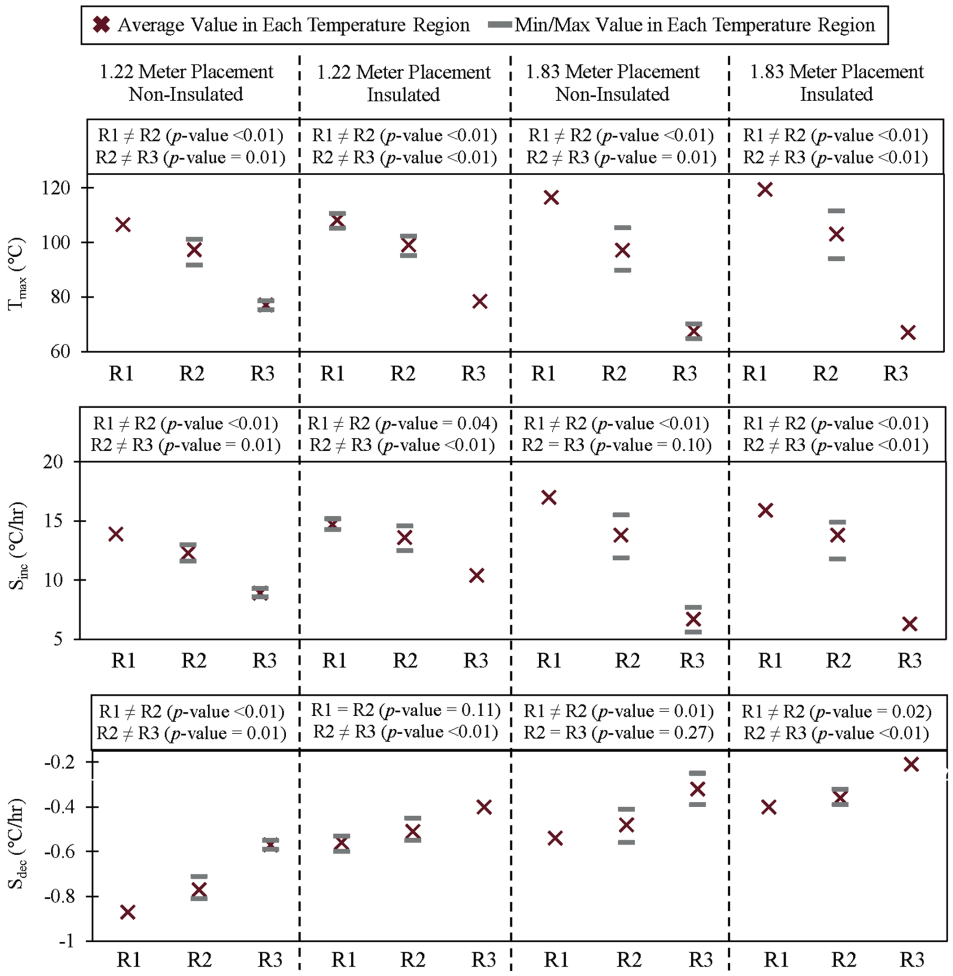

Fig. 7—Summary of t*-tests comparing maximum temperature (*T_{max}*),* S_{inc}*, and* S_{dec} *for R1 to R2 and R2 to R3 for each mass placement. (Note: °F = (9/5)(°C) + 32; 1 m = 3.28 ft.)*

based on one mixture, the three-stage method has the ability to account for different mixtures by adjusting key metrics.

Temperature profiles from R3 of each mass placement (that is, near the surface, where external temperatures can meaningfully influence time-temperature histories) were not accurately replicated. For all four placements, S_{inc}, T_{max}, and S_{dec} were statistically different than the laboratory protocol. The combination of insulation (PIR in the case of Fig. 7) as well as a programmed boundary condition produced temperatures that were much higher than measured mass placement temperatures. R3 three-stage protocols were also conducted using the AH curing block, which had a significantly lower insulating *R*-value than PIR. Even with the decreased insulating value, AH blocks produced time-temperature profiles that were meaningfully different than mass placement temperatures (Fig. 9). S_{inc} and T_{max} of PIR and AH blocks used with R3 curing protocols were similar, while S_{dec} was noticeably different. Although the three-stage protocol did not replicate time-temperature profiles of concrete near the edge of a mass placement, where external temperatures meaningfully influence temperatures, Stage 1 only shows interest in replicating R3 profiles, as discussed in the following paragraph.

Previous efforts reported by Carey et al.[8] evaluated and recommended two curing protocols for modestly sized UHPC placements with least dimensions between 0.15 and 0.50 m (0.5 and 1.6 ft). Laboratory specimens were cured with these recommended protocols and compared to R3 temperature profiles (Fig. 9). For 1.22 m (4 ft) placements, the PIR protocol (3 days in 23°C [73°F] ambient temperatures) reasonably replicated S_{inc} and T_{max} but did not replicate S_{dec} adequately. Although this PIR protocol overpredicted T_{max} of both 1.83 m (6 ft) placements, this laboratory protocol produced closer estimates of R3 mass placement temperatures. When evaluating the AH block protocol, T_{max} was overpredicted in all cases by 10 to 25°C (18 to 45°F). The PIR protocol is promising as this is currently being used as Stage 1 of the three-stage curing protocol, so R3 temperatures could potentially be approximated using Stage 1 of the proposed framework.

Mechanical properties evaluation

Sets of four specimens were tested after undergoing each of the 19 curing protocols. There is no core data from these mass placements to benchmark against; however, ranges of anticipated mechanical properties of the mass placements can be estimated using laboratory data. Although mechanical properties data from curing protocol 12 are reported in Table 5, they are not included in analysis of mechanical properties as the curing protocol failed.

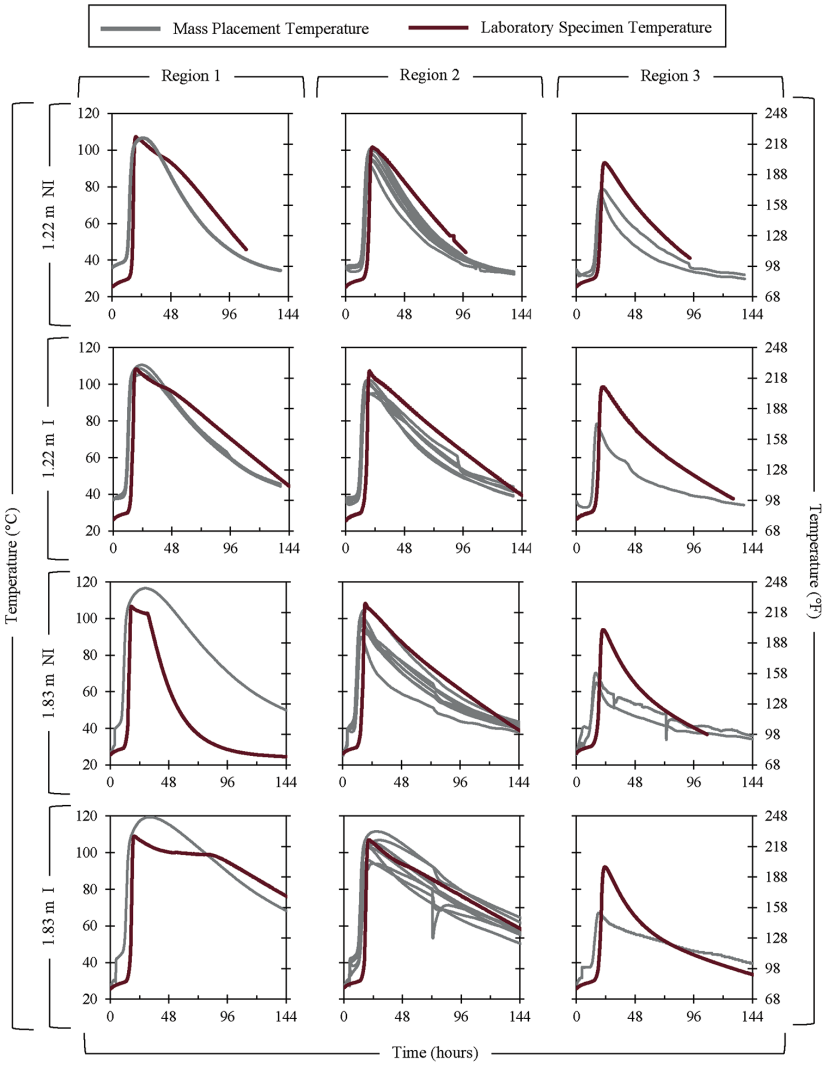

Fig. 8—Time-temperature profiles of mass placements compared to time-temperature profiles of laboratory-cured specimens. (Note: NI is non-insulated; I is insulated; 1 m = 3.28 ft.)

The f_c of laboratory specimens had noticeable variability, with almost 90% of curing protocols producing coefficient of variation (COV) values greater than 10%. ANOVA tests at a 0.05 significance level showed there was no statistical difference in mechanical properties from curing protocols that are intended to represent temperature regions in the non-insulated and insulated 1.22 m (4 ft) placements as well as the non-insulated 1.83 m (6 ft) placement (p-values of 0.72, 0.07, and 0.06, respectively). Although not significantly different, the insulated 1.22 m (4 ft) placement and non-insulated 1.83 m (6 ft) placement were very close to the 0.05 significance threshold. For the insulated 1.83 m (6 ft) placements, mechanical properties from each temperature region were statistically different (p-value = 0.01). Overall, these findings are encouraging as there was statistical significance identified between temperature curing protocols of mass placements and f_c. Future work is needed to compare core strengths of mass placements to strengths of laboratory specimens cured following the Fig. 1 three-stage framework.

Compressive strengths of mass placement curing protocols were also compared to traditional curing protocols. Specimens cured for 28 days in a 23°C (73°F) fog room produced an average f_c of 68 MPa (9860 psi), and 58% of specimens cured to replicate a mass placement were within ±10 MPa (1450 psi) of the 28-day f_c. Mass placement cured specimens were also benchmarked to specimens cured to what is believed by some to be near ultimate strength by curing at 23°C (73°F) for 7 days, followed by 7 days submerged in a 90°C (194°F) water bath. Ultimate strength specimens yielded an average f_c of 94 MPa (13,634 psi), which was meaningfully higher than all reported three-stage protocol cured specimen f_c, except for curing protocol 16 (1.83 m [6 ft] insulated placement; R1). This indicates that thermal treatment (similar to what is described in ASTM C1856/C1856M-17[16]) is likely not representative of strengths within some mass placements.

Linear regression analysis was conducted to determine the statistical relationships of calibration variables (for example, t_D, S_{inc}, t_{PD}, and S_{dec}) and f_c, similar to the analysis in Carey et al.[23] Each variable was compared to f_c, and statistically significant relationships were quantified for t_D (p-value <0.01) and t_{PD} (p-value of 0.05); however, there was not a statistical relationship for S_{inc} (p-value of 0.34) and S_{dec} (p-value of 0.26) (Table 6). This indicates that for the concrete

Table 5—Thermal and mechanical results of laboratory specimens

Curing protocol	Thermal variables			f_c			E		
	T_{max}, °C	S_{inc}, °C/h	S_{dec}, °C/h	n	Avg., MPa	COV, %	n	Avg., MPa	COV, %
1	89.5	12.7	–1.27	4	67	15.8	2	35,878	0.1
2	79.6	9.79	–1.26	4	75	11.8	2	38,380	0.7
3	108.7	17.8	–0.52	4	72	19.2	2	41,378	1.2
4	107.3	26.6	–0.76	4	64	29.8	2	43,010	13.6
5	101.7	19.0	–0.80	4	74	8.7	2	34,610	3.1
6	93.1	14.7	–0.77	4	74	13.0	2	36,136	4.9
7	87.2	14.7	–0.80	4	70	6.3	2	41,752	2.9
8	108.5	20.7	–0.55	4	49	22.6	2	27,374	14.6
9	107.3	22.2	–0.55	4	68	24.3	2	37,514	5.8
10	98.6	16.9	–0.59	4	73	15.8	2	37,928	6.9
11	100.8	18.5	–0.72	4	50	8.9	2	49,585	32.2
12*	—	—	—	3	36	9.2	1	41,172	—
13	108.2	20.0	–0.56	4	45	36.4	2	33,071	20.4
14	93.9	14.8	–0.76	4	67	15.7	2	37,270	1.2
15	85.6	13.4	–0.81	4	59	17.4	2	33,663	28.7
16	109.1	24.8	–0.31	4	95	8.5	2	35,941	3.9
17	107.0	23.3	–0.38	4	64	8.1	2	33,900	4.0
18	92.2	13.9	–0.59	4	80	20.1	2	37,760	17.2
19	85.9	14.0	–0.58	4	72	22.1	2	32,994	8.0

*Curing protocol 12 failed due to equipment limitations. Detailed thermal data are not available; mechanical properties shown as reference but are not included in analysis.

Note: T_{max} is maximum recorded internal specimen temperature; S_{inc} is rate of temperature increase recorded from specimen; S_{dec} is rate of temperature decrease recorded from specimen; f_c is unconfined compressive strength; E is elastic modulus; n is number of replicates; Avg. is average; 1 MPa = 145 psi; °F = (9/5)(°C) + 32.

evaluated herein, the programmed dormant periods statistically influenced f_c, while the programmed slopes (increase and decrease) had no statistical influence on f_c. More analysis is needed on a wide range of mixtures to fully quantify the influence of calibration variables on mechanical properties; however, this analysis shows that the recommended three-stage curing protocol does statistically influence mechanical properties, further highlighting its potential to characterize thermomechanical properties of modest to mass placements where HSCs are used.

The elastic modulus (E) was less variable than f_c, with only 33% of E values having a COV higher than 10%. ANOVA tests at a 0.05 significance level showed there were no statistical differences between E values from temperature regions for each placement (p-values of 0.18, 0.06, 0.47, and 0.68, respectively). Additionally, there were no statistically significant relationships between calibration variables and elastic modulus (Table 6). These findings align with previous research by the authors where, so long as naturally occurring hydration reactions occur (that is, delaying curing protocols until concrete has naturally begun hydration reactions), the elastic modulus is not significantly influenced by changes in curing temperature.[22]

CONCLUSIONS AND RECOMMENDATIONS

This paper focused on vetting a three-stage testing protocol that aims to cure laboratory specimens with a protocol that replicates temperature histories of a mass placement. From this work, the following conclusions can be drawn:

1. Recorded mass placement peak temperatures ranged from 107 to 119°C (225 to 246°F), which were higher than Table 1 reported temperatures and exceeded limits of equipment used by the authors.

2. The three-stage protocol was successful at replicating temperature profiles in regions where exterior temperatures do not play a meaningful role in the time-temperature history. Stage 1 curing procedures were shown to reasonably replicate temperature profiles near the edge.

3. There was a statistically significant relationship between calibration variables (that is, t_D and t_{PD}) used to develop three-stage curing protocols and compressive strength.

Based on these conclusions, the following recommendations with respect to the three-stage curing protocol evaluated herein are provided:

1. More robust and standardized equipment is needed to successfully recreate curing protocols at the extreme temperatures (that is, >115°C [239°F]) recorded in mass placements.

2. Although the upper temperature boundaries of the testing protocol are reasonably understood, more research is needed to quantify the potential of the three-step curing protocol for concretes that do not generate as much heat during hydration.

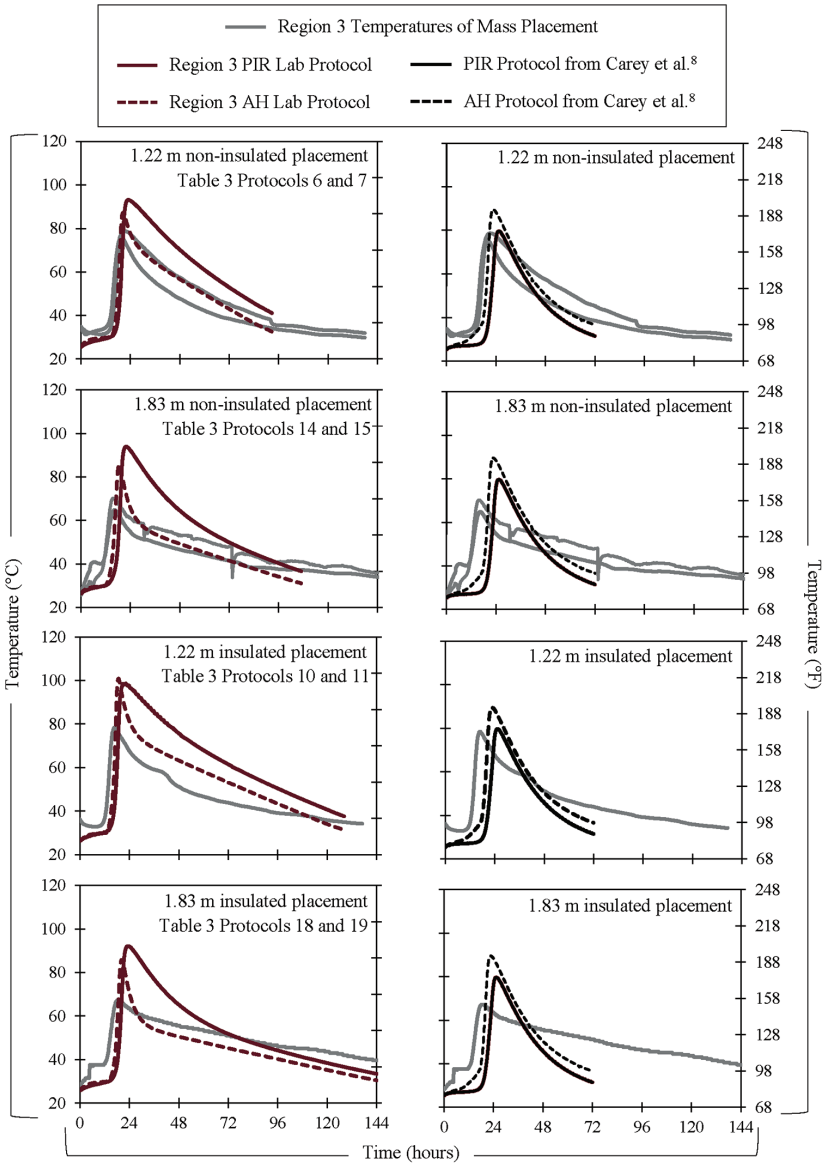

Fig. 9—Comparison of insulating block material and previously published curing protocols from Carey et al.[8] to R3 time-temperature profiles recorded herein. (Note: 1 m = 3.28 ft.)

Table 6—Relationships between calibration variables and mechanical properties

Variable 1	Variable 2	Equation	*p*-value on equation slope	Conclusions
f_c	t_D	$f_c = 6.04(t_D) - 0.34$	<0.01	Statistically significant
	S_{inc}	$f_c = -0.81(S_{inc}) + 78.0$	0.33	Not statistically significant
	t_{PD}	$f_c = 0.30(t_{PD}) + 62.0$	0.05	Statistically significant
	S_{dec}	$f_c = 15.9(S_{dec}) + 76.3$	0.26	Not statistically significant
E	t_D	$E = 1169(t_D) + 21{,}938$	0.14	Not statistically significant
	S_{inc}	$E = -350(S_{inc}) + 40{,}016$	0.28	Not statistically significant
	t_{PD}	$E = -18(t_{PD}) + 36{,}257$	0.76	Not statistically significant
	S_{dec}	$E = -3057(S_{dec}) + 34{,}351$	0.58	Not statistically significant

Note: t_D is length of dormant period in hours; S_{inc} is rate of temperature increase in °C/h; t_{PD} is length of peak temperature in hours; S_{dec} is rate of temperature decrease in °C/h; f_c is unconfined compressive strength in MPa; E is elastic modulus in MPa; p-value ≤ 0.05 indicates statistically significant relationship.

3. Test mass placements that can be cored to measure the in-place compressive strength (f_c) of the placement to compare to the laboratory testing framework.

4. Mass placements with a wide range of constituents should be evaluated within the framework to ensure its validity for multiple mixtures.

AUTHOR BIOS

Ashley S. Carey *is a former Research Engineer II at the Center for Advanced Vehicular Systems in Starkville, MS. She received her bachelor's, master's, and doctorate degrees from Mississippi State University (MSU), Starkville, MS, in 2017, 2019, and 2021, respectively. Her research interests include construction materials, with an emphasis on high-strength concretes and cement-stabilized materials.*

ACI member **Grayson B. Sisung** *is a Graduate Research Assistant at MSU, where she received her bachelor's and master's degrees in 2020 and 2023, respectively. Her research interests include high-strength concretes.*

ACI member **Isaac L. Howard** *is the Director of the Richard A. Rula School of Civil and Environmental Engineering at MSU. He received his bachelor's, master's, and doctorate degrees between 2001 and 2006 from Arkansas State University, Jonesboro, AR; West Virginia University, Morgantown, WV; and the University of Arkansas, Fayetteville, AR, respectively. His research interests include construction materials for infrastructure.*

ACI member **Brad Songer** *is a Research Civil Engineer at the U.S. Army Corps of Engineers Engineer Research and Development Center (ERDC) in Vicksburg, MS. He received his bachelor's degree from Jackson State University, Jackson, MS, in 2019. His research interests include mass concrete and high-strength concretes.*

ACI member **Dylan A. Scott** *is a Research Mechanical Engineer at ERDC. He received his bachelor's degree from the University of Mississippi, Oxford, MS, in 2012, and his master's degree from MSU in 2017. His research interests include high-performance, fiber-reinforced, and alternative-binder concretes.*

ACI member **Jay Shannon** *is the Chief of the Concrete and Materials Branch at ERDC. He received his bachelor's, master's, and doctorate degrees from MSU in 2011, 2012, and 2015, respectively. His research interests include cement and concrete chemistry and sustainability.*

ACKNOWLEDGMENTS

The work described herein was supported by the U.S. Army Engineer Research and Development Center (ERDC) and the Military Engineering Research and Development Area under Contract No. W912HZ-21C0022 (PE 0603119A; Project B03; "Military Engineering Tech Demonstrations"; Task 06). R. Moser was a key technical advisor and program manager. Any opinions, findings, and conclusions or recommendations expressed in this material are those of the authors and do not necessarily reflect the views of the U.S. Government. Permission was granted by the Director, Geotechnical and Structures Laboratory, to publish this information.

REFERENCES

1. ACI Committee 228, "Report on Methods for Estimating In-Place Concrete Strength (ACI 228.1R-19)," American Concrete Institute, Farmington Hills, MI, 2019, 48 pp.

2. ASTM C805/C805M-18, "Standard Test Method for Rebound Number of Hardened Concrete," ASTM International, West Conshohocken, PA, 2018, 4 pp.

3. ASTM C597-16, "Standard Test Method for Pulse Velocity Through Concrete," ASTM International, West Conshohocken, PA, 2016, 4 pp.

4. ASTM C873/C873M-15, "Standard Test Method for Compressive Strength of Concrete Cylinders Cast in Place in Cylindrical Molds," ASTM International, West Conshohocken, PA, 2015, 4 pp.

5. ASTM C1074-19, "Standard Practice for Estimating Concrete Strength by the Maturity Method," ASTM International, West Conshohocken, PA, 2019, 10 pp.

6. Riding, K.; Schindler, A.; Pesek, P.; Drimalas, T.; and Folliard, K., "ConcreteWorks V3 Training/User Manual (P1): ConcreteWorks Software (P2)," Report No. 0-6332-P1 and P2, Texas Department of Transportation, Austin, TX, 2017, 130 pp.

7. Carey, A. S.; Roberson, M. M.; Howard, I. L.; and Shannon, J., "Toward a Method to Predict Thermo-Mechanical Properties of High-Strength Concrete Placements," *Journal of Testing and Evaluation*, V. 52, No. 1, 2024, pp. 689-706. doi: 10.1520/JTE20220554

8. Carey, A. S.; Howard, I. L.; and Shannon, J., "Variable Temperature Insulated Block Curing on Laboratory Scale Specimens to Simulate Thermal Profiles of Modestly Sized Ultra-High Performance Concrete Placements," *Cement and Concrete Composites*, V. 133, 2022, Article No. 104707. doi: 10.1016/j.cemconcomp.2022.104707

9. Carey, A. S.; Howard, I. L.; Shannon, J.; Scott, D. A.; and Songer, B., "Laboratory Curing Protocols to Replicate Thermomechanical Behavior of High-Strength Concrete in Mass Placements," *Journal of Materials in Civil Engineering*, ASCE, V. 34, No. 8, 2022, p. 04022189. doi: 10.1061/(ASCE)MT.1943-5533.0004345

10. Riding, K. A.; Ferraro, C. C.; Hamilton, H. R.; Voss, M. S.; and Alrashidi, R. S., "Requirements for Use of Field-Cast, Proprietary Ultra-High-Performance Concrete in Florida Structural Applications," FDOT Contract No. BDV31-977-94, Florida Department of Transportation, Tallahassee, FL, 2019, 210 pp.

11. Kodur, V. K. R.; Bhatt, P. P.; Soroushian, P.; and Arablouei, A., "Temperature and Stress Development in Ultra-High Performance Concrete during Curing," *Construction and Building Materials*, V. 122, 2016, pp. 63-71. doi: 10.1016/j.conbuildmat.2016.06.052

12. Sbia, L. A.; Peyvandi, A.; Harsini, I.; Lu, J.; Ul Abideen, S.; Weerasiri, R. R.; Balachandra, A. M.; and Soroushian, P., "Study on Field Thermal Curing of Ultra-High-Performance Concrete Employing Heat of Hydration," *ACI Materials Journal*, V. 114, No. 5, Sept.-Oct. 2017, pp. 733-743. doi: 10.14359/51689677

13. Li, S.; Cheng, S.; Mo, L.; and Deng, M., "Effects of Steel Slag Powder and Expansive Agent on the Properties of Ultra-High Performance Concrete (UHPC): Based on a Case Study," *Materials*, V. 13, No. 3, 2020, Article No. 683. doi: 10.3390/ma13030683

14. Soliman, N. A.; Omran, A. F.; and Tagnit-Hamou, A., "Laboratory Characterization and Field Application of Novel Ultra-High-Performance Glass Concrete," *ACI Materials Journal*, V. 113, No. 3, May-June 2016, pp. 307-316. doi: 10.14359/51688827

15. Aghdasi, P.; Heid, A. E.; and Chao, S.-H., "Developing Ultra-High-Performance Fiber-Reinforced Concrete for Large-Scale Structural Applications," *ACI Materials Journal*, V. 113, No. 5, Sept.-Oct. 2016, pp. 559-570. doi: 10.14359/51689103

16. ASTM C1856/C1856M-17, "Standard Practice for Fabricating and Testing Specimens of Ultra-High Performance Concrete," ASTM International, West Conshohocken, PA, 2017, 4 pp.

17. Riding, K. A.; Poole, J. L.; Schindler, A. K.; Juenger, M. C. G.; and Folliard, K. J., "Evaluation of Temperature Prediction Methods for Mass Concrete Members," *ACI Materials Journal*, V. 103, No. 5, Sept.-Oct. 2006, pp. 357-365.

18. Gross, E. D.; Eiland, A. D.; Schindler, A. K.; and Barnes, R. W., "Temperature Control Requirements for the Construction of Mass Concrete Members," Report No. 930-860R, Highway Research Center, Auburn, AL, 2017, 248 pp.

19. ACI Committee 207, "Mass Concrete—Guide (ACI PRC-207.1-21)," American Concrete Institute, Farmington Hills, MI, 2021, 34 pp.

20. Binard, J. P., "UHPC: A Game-Changing Material for PCI Bridge Producers," *PCI Journal*, V. 62, No. 2, 2017, pp. 34-46. doi: 10.15554/pcij62.2-01

21. Heinz, D., and Ludwig, H.-M., "Heat Treatment and Risk of DEF Delayed Ettringite Formation in UHPC," *Ultra High Performance Concrete (UHPC): Proceedings of the International Symposium*, M. Schmidt, E. Fehling, and C. Geisenhanslüke, eds., Kassel, Germany, 2004, pp. 717-730.

22. Allard, T. E.; Carey, A. S.; Howard, I. L.; and Shannon, J., "Time-Temperature Implications of Curing on Mechanical Properties of Ultra-High-Performance Concrete," *ACI Materials Journal*, V. 119, No. 5, Sept. 2022, pp. 251-260. doi: 10.14359/51735978

23. Carey, A. S.; Howard, I. L.; and Shannon, J., "Effects of Silica Fume Purity on Behavior of Ultra-High Performance Concrete," *Advances in Civil Engineering Materials*, V. 11, No. 1, 2022, pp. 354-371. doi: 10.1520/ACEM20220017